

Radon transform and multiple attenuation

Zhihong (Nancy) Cao, John C. Bancroft, R. James Brown, and Chunyan (Mary) Xaio

ABSTRACT

Removing reverberations or multiples from reflection seismograms has been a longstanding problem of exploration geophysics. Multiple reflections often destructively interfere with the primary making interpretation difficult. The Radon transform, which integrates some physical property along a particular path, will be evaluated for attenuating multiple.

Multiples are periodic in the τ - p domain, and predictive deconvolution can be applied in the τ - p domain to suppress multiples. After NMO correction, moveout errors are approximately parabolic and tend to map to points in the parabolic Radon domain. The hyperbolic Radon transform will also map data before and after moveout correction into points, and multiples can be recognized in the Radon domain. The identified multiple energy can then be subtracted from the data to improve the interpretation process.

INTRODUCTION

Johan Radon (1917) is credited with establishing the Radon transform, a function that integrates some physical property of a medium along a particular path.

Removing reverberations from reflection seismograms has been a long standing problem of exploration geophysics. Multiple reflections often destructively interfere with the primary reflections of interest. The most robust and effective way to suppress multiples is stacking normal moveout (NMO) corrected seismic gathers (Foster and Mosher, 1992). Unfortunately, stacking does not eliminate all multiples.

Over the years, many techniques for suppressing multiples have been tried. More recently, the Radon transform approaches have attracted attention. The generalized Radon transform integrates the data along any curved surfaces (Chapman, 1981). Particularly, the slant-stack (or τ - p) transform integrates the data along planar surfaces (Treitel, et al, 1982). Hampson (1986) applied NMO-correction to common midpoint (CMP) data and perform a Radon transform along parabolic stacking curve to suppress multiples in NMO-corrected domain. Yilmaz (1989) applied t^2 -stretching to the CMP data and then applied the parabolic Radon transform in the stretched coordinates. Foster and Mosher (1992) described a hyperbolic Radon transform in stacking NMO-corrected domain. Oppert (2002) proposed the non-hyperbolic Radon transform by taking the shifted hyperbola NMO equations. Thorson and Claerbout (1985), and Beylkin (1987) showed the least-squares solution of the discrete Radon transform. The former also gave the

stochastic inverse solution for the problem. Zhou and Greenhalgh (1994) showed the convolutional operators for the slant-stack transform and the parabolic Radon transform to increase the resolution. Sacchi and Tadeusz (1995) proposed an improved algorithm for the parabolic Radon transform to get higher resolution.

The generalized Radon transform $u(q, \tau)$ is defined as

$$u(q, \tau) = \int_{-\infty}^{\infty} d(x, t = \tau + q\phi(x)) dx, \quad (1)$$

where $d(x, t)$ is the original seismogram, x is a spatial variable such as offset, $\phi(x)$ is the curvature based on which the transform curve is defined, q is the slope of the curvature, and τ is the intercept time (Foster and Mosher, 1992).

Since the seismogram is digitally recorded, a discrete form of equation (1) is:

$$u(q, \tau) = \sum_x d(x, t = \tau + q\phi(x)), \quad (2)$$

Then the inverse transforms of equation (1) and (2) are:

$$d'(x, t) = \int_{-\infty}^{\infty} u(q, \tau = t - q\phi(x)) dq, \quad (3)$$

or

$$d'(x, t) = \sum_q u(q, \tau = t - q\phi(x)), \quad (4)$$

Also, we can express the Radon transform in velocity domain (Yilmaz, 1989) as follows:

$$u(v, \tau) = \sum_x d(x, t = \tau + q\phi(v, x)), \quad (5)$$

$$d'(x, t) = \sum_q u(v, \tau = t - q\phi(v, x)), \quad (6)$$

THE DISCRETE RADON TRANSFORM

Equation (3) can be written as:

$$\mathbf{d}' = \mathbf{L}\mathbf{u}, \quad (7)$$

where \mathbf{L} is the linear transformation from the τ - q space to the offset space defined by equation (3), and given as follows in Fourier domain:

$$\mathbf{L}_{jk} = e^{-i\omega q_j \phi(x_k)} \begin{cases} j = 1, \dots, M \\ k = 1, \dots, N \end{cases}, \quad (8)$$

Assume that a CMP gather $d(x,t)$ is the result of some transform on a function $u_0(q, \tau)$ in the τ - q space. In fact, $d(x,t)$ is always contaminated with additive noise \mathbf{n} giving:

$$\mathbf{d} = \mathbf{L}\mathbf{u}_0 + \mathbf{n}, \quad (9)$$

The solution for \mathbf{u} in equation (9) is obtained by taking a least-squares approach to minimize the noise term \mathbf{n} , which represents the difference between the actual data \mathbf{u}_0 and the modelled data \mathbf{u} . The cumulative squared noise term, $\mathbf{S} = \mathbf{n}^T \mathbf{n} = (\mathbf{d} - \mathbf{L}\mathbf{u}_0)^T (\mathbf{d} - \mathbf{L}\mathbf{u}_0)$ (Oppert and Brown, 2002), is minimized with respect to \mathbf{u}_0 yielding the desired least-squares solution (Thorson and Claerbout, 1985):

$$\mathbf{u} = [\mathbf{L}^T \mathbf{L}]^{-1} \mathbf{L}^T \mathbf{d}, \quad (10)$$

The generalized inverse of \mathbf{L} is thus computed to be $[\mathbf{L}^T \mathbf{L}]^{-1} \mathbf{L}^T$.

The calculation of $[\mathbf{L}^T \mathbf{L}]^{-1}$ is impractical due to the large nature of the matrix and the instability of the inversion. Although the operator $\mathbf{L}^T \mathbf{L}$ is diagonally dominant, if the side lobes of the matrix are significant, smearing will occur along the q -axis. Prewhitening the operator $\mathbf{L}^T \mathbf{L}$ suppresses the side lobes and stabilizes the inversion. A stable solution for equation (9) is computed by Thorson and Claerbout (1985):

$$\mathbf{u} = [\mathbf{L}^T \mathbf{L} + \mu \mathbf{I}]^{-1} \mathbf{L}^T \mathbf{d}, \quad (11)$$

where the constant μ is a damping factor incorporated to add white noise along the main diagonal of the inversion matrix, and \mathbf{I} is the identity matrix.

THE LINEAR RADON TRANSFORM

Theory

$$u(p, \tau) = \int_{-\infty}^{\infty} d(x, t = \tau + px) dx, \quad (12)$$

$$u(p, \tau) = \sum_x d(x, t = \tau + px), \quad (13)$$

$$d'(x, t) = \int_{-\infty}^{\infty} u(p, \tau = t - px) dp, \quad (14)$$

$$d'(x, t) = \sum_p u(p, \tau = t - px), \quad (15)$$

The equation (1) reduces to the linear Radon transform when $\phi(x) = x$, where x is offset. Accordingly, equations (1) to (4) are reformatted as equations (12) to (15).

For seismic exploration applications, $d(x, t)$ can be CMP or shot gather. $u(p, \tau)$ is its slant-stack transform with horizontal slowness (or ray parameter) p and intercept time τ . Here p is used because of its specific meaning of ray parameter and is defined by

$$p = \frac{\sin \theta}{v} = \frac{\Delta t}{\Delta x}, \quad (16)$$

where θ is the incident angle from the vertical axis, v is the wave propagation velocity.

The *rho* filter has to be applied before inverse mapping to restore the correct amplitude and phase. This work was illustrated by Zhou and Greenhalgh (1994).

The Fourier transform of equation (12) becomes

$$U(p, \omega) = \int_{-\infty}^{\infty} D(x, \omega) e^{i\omega px} dx, \quad (17)$$

Version 1:

To obtain the proper inverse transform $D(x, \omega)$ in equation (16), the standard back-projection $D'(x, \omega)$ is used:

$$\begin{aligned} D'(x, \omega) &= \int_{-\infty}^{\infty} U(p, \omega) e^{-i\omega px} dp = \int_{-\infty}^{\infty} \int_{-\infty}^{\infty} D(x', \omega) e^{i\omega p(x'-x)} dx' dp, \\ &= \int_{-\infty}^{\infty} dx' D(x', \omega) \int_{-\infty}^{\infty} e^{-i\omega p(x-x')} dp \end{aligned} \quad (18)$$

Now the rho filter is introduced:

$$\rho(x, \omega) = \int_{-\infty}^{\infty} e^{-i\omega p x} dp, \quad (19)$$

Then equation (17) can be written as:

$$D'(x, \omega) = \int_{-\infty}^{\infty} D(x', \omega) \rho(x - x', \omega) dx' = D(x, \omega) * \rho(x, \omega), \quad (20)$$

Here, “*” stands for convolution with respect to the spatial variable x . Zhou and Greenhalgh (1994) derive the form of rho filter in case of infinite p :

$$\rho(x, \omega) = \frac{2\pi}{|\omega|} \delta(x), \quad (21)$$

Substituting equation (21) to equation (20), we have

$$D'(x, \omega) = \frac{2\pi}{|\omega|} D(x, \omega)$$

or

$$D(x, \omega) = \frac{|\omega|}{2\pi} D'(x, \omega), \quad (22)$$

Therefore the slant-stack transform pair in the frequency domain is

$$\begin{cases} U(p, \omega) = \int_{-\infty}^{\infty} D(x, \omega) e^{i\omega p x} dx \\ D(x, \omega) = \frac{|\omega|}{2\pi} \int_{-\infty}^{\infty} U(\omega, p) e^{-i\omega p x} dp \end{cases}, \quad (23)$$

But in practice, variable p has a limited range of $[p_{\min}, p_{\max}]$. In this case, the rho filter becomes:

$$\rho(x, \omega) = \int_{p_{\min}}^{p_{\max}} e^{-i\omega p x} dp = \begin{cases} \frac{1}{i\omega x} (e^{-i\omega p_{\min} x} - e^{-i\omega p_{\max} x}), & \omega x \neq 0 \\ p_{\max} - p_{\min}, & \omega x = 0 \end{cases}, \quad (24)$$

When $p_{\min} = p_{\max}$, the equation (24) becomes a sinc function:

$$\rho(x, \omega) = \begin{cases} 2p_{\max} \left[\frac{\sin(\omega p_{\max} x)}{\omega p_{\max} x} \right], & \omega x \neq 0 \\ 2p_{\max}, & \omega x = 0 \end{cases}, \quad (25)$$

Version 2:

Zhou and Greenhalgh (1994) indicate that we can perform the inverse τ - p transform first and then the forward transform to derive the proper inversion of the slant-stack transform. The inverse τ - p transform and its Fourier transform are defined as:

$$d(x, t) = \int_{-\infty}^{\infty} u(p, t - px) dp, \quad (26)$$

and

$$D(x, \omega) = \int_{-\infty}^{\infty} U(p, \omega) e^{-i\omega px} dp, \quad (27)$$

Here $d(x, t)$ is the input data and $u(p, \tau)$ is the τ - p transform. $D(x, \omega)$ and $U(p, \omega)$ are the Fourier transforms of $d(x, t)$ and $u(p, \tau)$, respectively. To obtain the forward τ - p transform $U(p, \omega)$ in equation (26), $U'(p, \omega)$ is defined as:

$$\begin{aligned} U'(p, \omega) &= \int_{-\infty}^{\infty} D(x, \omega) e^{i\omega px} dx \\ &= \int_{-\infty}^{\infty} dp' U(p', \omega) \int_{-\infty}^{\infty} e^{i\omega x(p-p')} dx \end{aligned}, \quad (28)$$

The new function $g(p, \omega)$ is introduced:

$$g(p, \omega) = \int_{-\infty}^{\infty} e^{i\omega px} dx, \quad (29)$$

Then equation (28) can be written as:

$$U'(p, \omega) = U(p, \omega) * g(p, \omega), \quad (30)$$

In case that the spatial variable x is of infinite range, we have:

$$g(p, \omega) = \frac{2\pi}{|\omega|} \delta(p), \quad (31)$$

The τ - p transform pair in the frequency domain can be written as

$$\begin{cases} U(p, \omega) = \frac{|\omega|}{2\pi} \int_{-\infty}^{\infty} D(h, \omega) e^{i\omega p x} dx \\ D(x, \omega) = \int_{-\infty}^{\infty} U(p, \omega) e^{-i\omega p x} dp \end{cases}, \quad (32)$$

In case that the spatial variable x is of finite range $[x_{min}, x_{max}]$, we have $g(p, \omega)$:

$$g(p, \omega) = \begin{cases} \frac{1}{i\omega p} (e^{i\omega x_{max} p} - e^{i\omega x_{min} p}), & \omega p \neq 0 \\ x_{max} - x_{min}, & \omega p = 0 \end{cases}, \quad (33)$$

If $x_{min} = -x_{max}$, $g(p, \omega)$ can be written as:

$$g(h, \omega) = \begin{cases} 2h_{max} \left[\frac{\sin(\omega p h_{max})}{\omega p h_{max}} \right], & \omega h \neq 0 \\ 2h_{max}, & \omega h = 0 \end{cases}, \quad (34)$$

Comparing the two versions of the linear τ - p transforms, i.e. equation (23) and equation (32), the only difference is that the deconvolution in version 1 is performed on the inverse transform in x -direction, and that the deconvolution in version 2 is performed on the forward transform in p -direction. Deconvolution can improve resolution in the x -direction for version 1 and in p -direction for version 2. In order to attenuate noise in the τ - p domain, the transform pair of version 2 is preferred (Zhou and Greenhalgh, 1994).

Slant-stack multiple attenuation

For a one-layer model with velocity v , the travelttime equation in offset domain is:

$$t^2 = t_0^2 + \frac{x^2}{v^2}, \quad (35)$$

where x is the source/receiver offset and t_0 is the two-way zero-offset time.

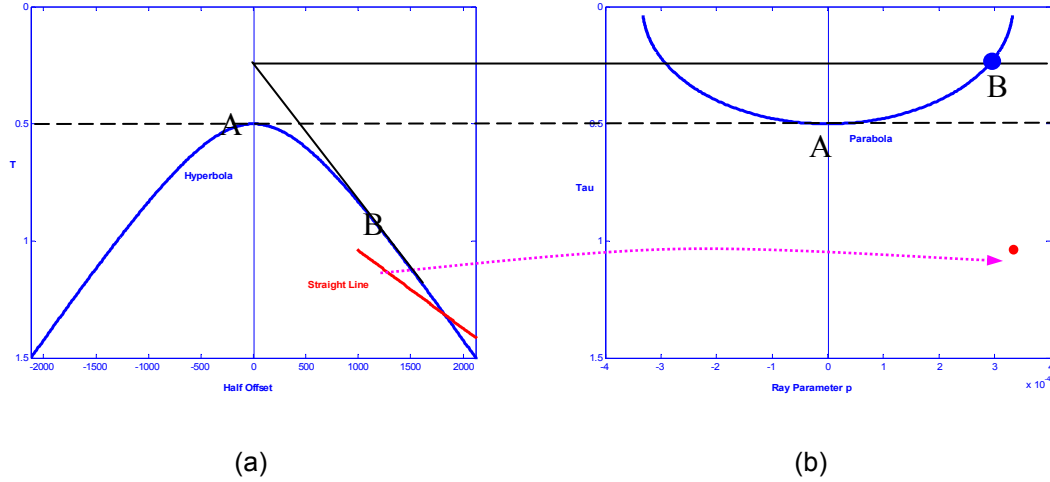


FIG. 1. A hyperbola in CMP gather (a) maps onto an ellipse in the slant-stack domain (b); and a straight line in CMP gather maps to and a point in the slant-stack domain. Energy tangent to the line B in (a) maps to the point B in (b).

In the slant-stack domain, equation (35) is transformed to (Alam and Austin, 1981):

$$\tau^2 = (1 - p^2 v^2) \tau_0^2, \quad (36)$$

Comparing equation (35) with (36) we see that the hyperbola in the (x, t) domain becomes an ellipse in the (τ, p) domain. The linear events in the offset space map to points in the (τ, p) space (Figure 1). But notice the ellipse in Figure 1b that the ellipse is incomplete because the offset, in practice, couldn't be infinite. So when the data maps from τ - p domain back to the offset domain, amplitude smearing will occur.

Now consider the traveltime for an n -bounce multiple in (τ, p) domain and time delay between successive bounces for a given trace (Alam and Austin, 1981):

$$\tau^2 = (1 - p^2 v^2) n^2 \tau_0^2, \quad (37)$$

$$\tau_n - \tau_{n-1} = (1 - p^2 v^2)^{\frac{1}{2}} \tau_0, \quad (38)$$

Multiples are not periodic in the offset domain. Taner (1980) first recognized that the time separations between the arrivals are equal along a radial direction OR in the offset space (Figure 2). Then Alam and Austin (1981) showed in equation (38) that all bounces within a reverberatory layer have the same traveltime for a given p -value, i.e. the multiples are exactly periodic in the (τ, p) space (Figure 2).

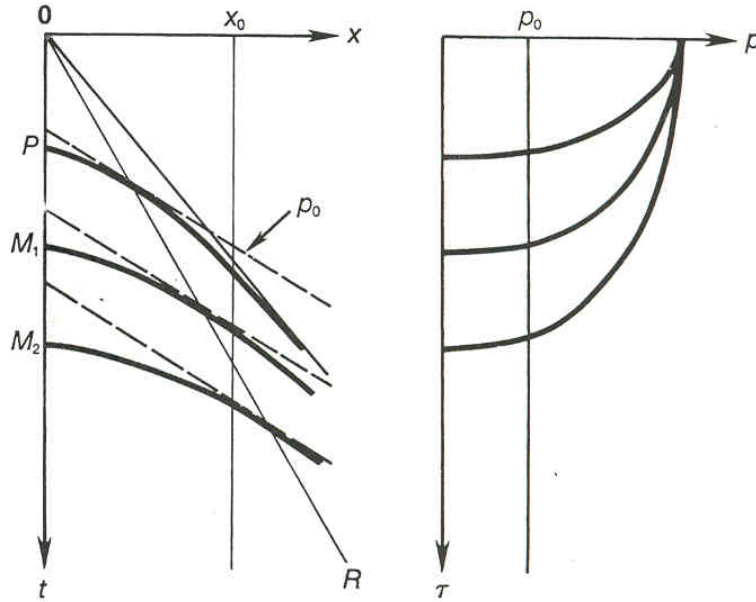


FIG. 2. The periodicity of multiples along radial trace OR and down p traces from Taner (1980).

Based on the periodic property of the multiples in the (τ, p) domain, Alam and Austin (1981) and Treitel et al. (1982) investigated the application of predictive deconvolution in the slant-stack domain for multiple suppression. The shot gather in Figure 3a is transformed to the slant-stack domain (Figure 3c). Figure 3e is the slant-stack gather after predictive deconvolution. Figure 3b, d, and f are the autocorrelations of Figure 3a, c and e, respectively. Figure 3g shows the reconstruction of the shot gather from the slant-stack gather in Figure 3e. Unlike the autocorrelogram of the shot gather in Figure 3b, the periodic nature of the multiples in the data is pronounced in the autocorrelogram of the slant-stack gather (Figure 3d). Note that the periodicity of multiples changes from one p trace to the next. The largest period occurs along the trace that corresponds to the minimum p value. The autocorrelogram after predictive deconvolution shows that the energy in lags less than the specified prediction lag is retained, while the multiple energy is attenuated (Figure 3f) (Yilmaz, 1989).

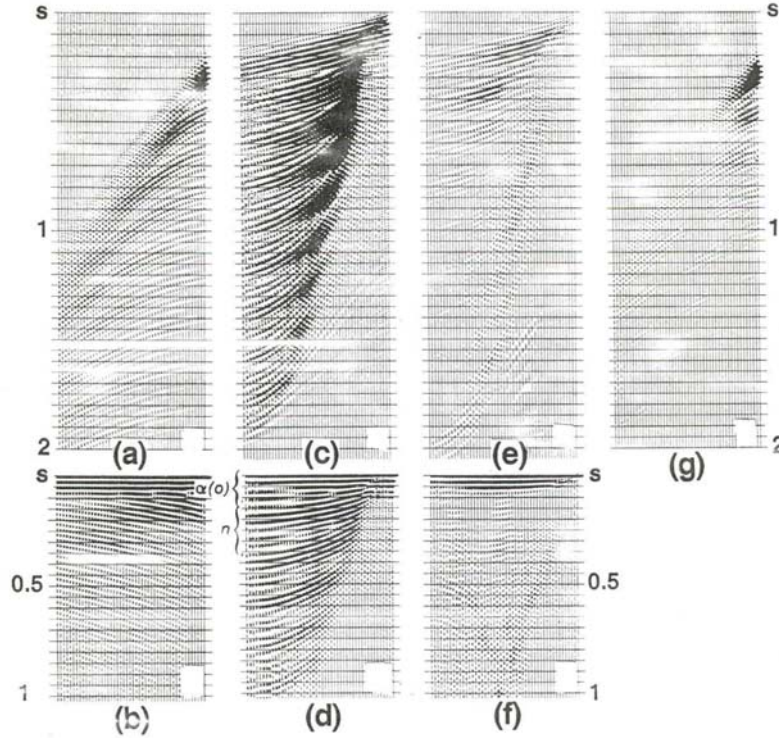


FIG. 3. Multiple attenuation in the slant-stack domain (a) A shot gather; (b) Autocorrelogram of (a); (c) The slant-stack gather; (d) The autocorrelogram of (c); (e) The slant-stack gather after predictive deconvolution, where operator length=240 ms; (f) The autocorrelogram of (e); (g) Reconstruction of the shot gather from (e) given by Yilmaz (1987).

THE PARABOLIC RADON TRANSFORM

Theory

On CMP or common shotpoint CSP gathers, seismic events are more likely to be hyperbolic than linear (reflections and diffractions are hyperbolic, but refractions and direct waves are linear). A hyperbolic Radon transform can be designed so that the hyperbolic events in the seismic domain map into points in the Radon domain. But the direct hyperbolic τ - p transform was too expensive to realize and faster method were sought. Errors in the moveout correction due to velocity approximations are exactly hyperbolic, but their small amounts of curvature may be approximated by parabolas. Consequently Hampson (1986) performed the parabolic Radon transform on the NMO-corrected offset data. Yilmaz (1989) noted that all the hyperbolic events in the offset domain are transformed to exact parabolas after t^2 -stretch is applied.

NMO-corrected input data

A practical approach was presented by Hampson (1986). First, the input CMP gather is NMO-corrected using the hyperbolic moveout equation

$$t_n = \sqrt{t^2 - \frac{x^2}{v_n^2}}, \quad (39)$$

where t is the recorded time, t_n is the time after NMO-correction, and v_n is the NMO-correction velocity. The resulting moveout of the events, which were originally hyperbolic, are now approximately parabolic:

$$t^2 = t_0^2 + \frac{x^2}{v^2} \quad (40)$$

$$t_{err}^2 = t_0^2 + \frac{x^2}{v_{err}^2} \quad (41)$$

$$t_{err}^2 = t^2 - \frac{x^2}{v^2} + \frac{x^2}{v_{err}^2}, \text{ error term is exactly hyperbolic} \quad (42)$$

$$\frac{t_{err}^2}{t^2} = 1 + \frac{x^2}{t^2} \left(\frac{1}{v_{err}^2} + \frac{1}{v^2} \right) \quad (43)$$

$$\frac{t_{err}}{t} = \sqrt{1 + \frac{x^2}{t^2} \left(\frac{1}{v_{err}^2} + \frac{1}{v^2} \right)} \quad (44)$$

$$\frac{t_{err}}{t} \approx 1 + \frac{x^2}{2t^2} \left(\frac{1}{v_{err}^2} + \frac{1}{v^2} \right) \quad (45)$$

$$t_{err} \approx t + \frac{x^2}{2t} \left(\frac{1}{v_{err}^2} + \frac{1}{v^2} \right), \text{ approximately parabolic} \quad (46)$$

$$t_n = \tau + qx^2, \quad (47)$$

where τ is the two-way zero-offset time, and q defines the curvature of the parabola.

Say $d(x, t_n)$ is the NMO-corrected gather. The forward and inverse Radon transform in the NMO-corrected coordinates take the forms

$$u(q, \tau) = \sum_x d(x, t_n = \tau + qx^2), \quad (48)$$

and

$$d'(x, t) = \sum_q u(q, \tau = t_n - qx^2). \quad (49)$$

Stretching input data

Events on the CMP gather have hyperbolic traveltimes defined by

$$t^2 = \tau^2 + x^2/v^2, \quad (50)$$

where t is the two-way traveltime, τ is the two-way zero-offset traveltime, x is the offset, and v is the stacking velocity.

Apply stretching in the time direction by setting $t' = t^2$ and $\tau' = \tau^2$. Equation (50) takes the form

$$t' = \tau' + x^2/v^2, \quad (51)$$

From equation (51) we can see that the hyperbolae are transformed exactly to parabolae in the stretched coordinates. Now say $d(x, t')$ is the t'^2 -stretched input data. The mapping from the x - t' domain to the τ' - q space is achieved by summing over offset:

$$u(q, \tau') = \int_{-\infty}^{\infty} d(x, t' = \tau' + qx^2) dx,$$

or

$$u(q, \tau') = \sum_x d(x, t' = \tau' + qx^2), \quad (52)$$

And the inverse transforms are

$$d'(x, t') = \int_{-\infty}^{\infty} u(q, \tau' = t' - qx^2) dq,$$

or

$$d'(x, t') = \sum_q u(q, \tau' = t' - qx^2), \quad (53)$$

From equation (51), we know that the physical meaning of q is taken as the square of the horizontal slowness, or the inverse of the square of stacking velocity (Yilmaz, 1989). But, in practice, equation (53) doesn't give the exact inversion of the Radon transform.

To obtain superior image resolution in the transform domain, a similar approach as was used with the linear Radon transform, version 2, is taken in the following derivation of the parabolic τ - q transform. Now we take the Radon transform in the t^2 -stretching domain as an example, i.e. equations (52) and (53).

Say $D(x, \omega')$ and $U(q, \omega')$ are the Fourier transforms of $d(x, t')$ and $u(q, \tau')$, respectively. $D'(x, \omega')$ is the standard Fourier transform of the reverse parabolic Radon transform. Then, in the frequency domain, we have (Zhou and Greenhalgh, 1994):

$$D(x, \omega') = \int_{-\infty}^{\infty} U(q, \omega') e^{-i\omega'qx^2} dq, \quad (54)$$

The forward projection function $U'(x, \omega')$ of the parabolic τ - q transform is:

$$U'(q, \omega') = \int_{-\infty}^{\infty} D(x, \omega') e^{i\omega'qx^2} dx, \quad (55)$$

Substituting equation (54) to (55), we can get:

$$\begin{aligned} U'(q, \omega') &= \int_{-\infty}^{\infty} \int_{-\infty}^{\infty} U(q', \omega') e^{i\omega'x^2(q-q')} dq' dx \\ &= \int_{-\infty}^{\infty} dq' U(q', \omega') \int_{-\infty}^{\infty} e^{i\omega'x^2(q-q')} dx \end{aligned}, \quad (56)$$

The function $\sigma(q, \omega')$ defined by:

$$\sigma(q, \omega') = \int_{-\infty}^{\infty} e^{i\omega'qx^2} dx, \quad (57)$$

is introduced. Then equation (56) can be written as:

$$U'(q, \omega') = U(q, \omega') * \sigma(q, \omega'), \quad (58)$$

In case of infinite spatial input data, Zhou and Greenhalgh (1994) derived $\sigma(q, \omega')$ as:

$$\sigma(q, \omega') = [1 + i \operatorname{sign}(q)] \sqrt{\frac{\pi}{2\omega'|q|}}, \quad (59)$$

Equation (59) indicates that q -direction deconvolution is required even if the input data have an infinite spatial extent. This is different from the linear Radon transform, version 2. In the Fourier transform domain, equation (58) becomes:

$$U'(k_q, \omega') = U(k_q, \omega') \sigma(k_q, \omega'), \quad (60)$$

or

$$U(k_q, \omega') = \frac{U'(k_q, \omega')}{\sigma(k_q, \omega')} = \frac{\sqrt{\omega'} U'(k_q, \omega')}{\sigma'(k_q)}, \quad (61)$$

Here the new function $\sigma'(k_q)$ is given by Zhou and Greenhalgh (1994):

$$\begin{aligned} \sigma'(k_q) &= \int_{-\infty}^{\infty} [1 + i \operatorname{sign}(q)] \sqrt{\frac{\pi}{2|q|}} e^{-ik_q q} dq \\ &= [1 + i \operatorname{sign}(q)] \frac{\pi}{\sqrt{|k_q|}}, \end{aligned} \quad (62)$$

In fact, the Fourier transform variable k_q corresponding to variable q is positive. Therefore, equation (62) can be written as:

$$\sigma'(k_q) = \frac{2\pi}{\sqrt{|k_q|}}, \quad (63)$$

and equation (61) becomes:

$$U(k_q, \omega') = \frac{\sqrt{\omega k_p}}{2\pi} U'(k_q, \omega'), \quad (64)$$

which shows that the q -direction deconvolution enhances the Fourier transform components. Therefore the resolution in the parabolic τ - p transform domain is increased.

In case that the variable x has a limited range, $[x_{\min}, x_{\max}]$, there is no analytical solution for the equation (57), unless $\omega' = 0$, in which case $\sigma(q, \omega') = x_{\min} - x_{\max}$. This integral has to be approximated by numerical quadrature methods such as the rectangular, trapezoidal or Simpson rules.

Velocity-stack

We can do the parabolic Radon transform in the velocity domain. Then equation (52) and equation (53) can be written (Yilmaz, 1989) as:

$$u(v, \tau') = \sum_x d(x, t' = \tau' + 4x^2/v^2), \quad (65)$$

$$d'(x, t') = \sum_q u(v, \tau' = t' - 4x^2/v^2), \quad (66)$$

We have seen that equation (66) can't give the exact inversion of equation (65). So a *rho* filter is convoluted to $u(v, \tau')$ before integration over velocity (Beylkin, 1987):

$$d'(x, t') = \int_{-\infty}^{\infty} \rho(\tau) * u(v, \tau' = t' - 4x^2/v^2) dv, \quad (67)$$

where $\rho(\tau)$ has a Fourier transform of the form $\sqrt{\omega} \exp(i\pi/4)$.

In this case, \mathbf{L} , the linear transform [Equation (8)] from the velocity space to the offset space is modified as:

$$\mathbf{L}_{jk} = e^{-i\alpha x_j^2/v_k^2} \begin{cases} j = 1, \dots, M \\ k = 1, \dots, N \end{cases}, \quad (68)$$

Multiple Suppression

Since the mapping function is summed along parabolic curve, a parabola in the t^2 -space domain, such as a primary or multiple, ideally maps onto a point in the τ - q or Radon domain. Figure 4 (Yilmaz, 1989) shows primaries and multiples in the offset domain and the velocity domain. Those multiples have same velocity with their related primaries. Hence, we are able to distinguish multiples from primaries in the velocity domain based on velocity discrimination and attenuate multiples.

Now we take the velocity-stack transform into practice (Yilmaz, 1989). Figure 5a is a synthetic CMP gather with three primary reflections; 5b is a synthetic CMP gather with one primary reflection (arrival time at 0.2 s at zero-offset trace) and its multiples; 5c integrates 5a and 5b; 5d is the t^2 -stretching section of 5c. In Figure 6a is the velocity stack of Figure 5d; 6b is the velocity-stack after undoing t^2 -stretching, here we can separate multiples and primaries based on velocity differences as indicated; 6c is the full CMP gather reconstruction from 6b. Comparing Figure 6b with Figure 5d, Figure 6b is a reasonably good reconstruction. On Figure 7c, only primaries are reconstructed from

Figure 6b and there is some residual multiple energy. In practice, non-hyperbolic events, such as direct and refracted wave, will be lost during the parabolic Radon transform. So on Figure 7b, only multiples are constructed from Figure 6b. Then these multiples are subtracted from the original data Figure 5c, and all of those events aside from multiples are left on the output. On Figure 6b, we find some distortion of the wavelet in shallow events (less than 1 s). This is caused by t^2 -stretching. This distortion will produce blurry events in the offset domain, correspondingly, such as Figure 6c, 7a, 7b and 7c.

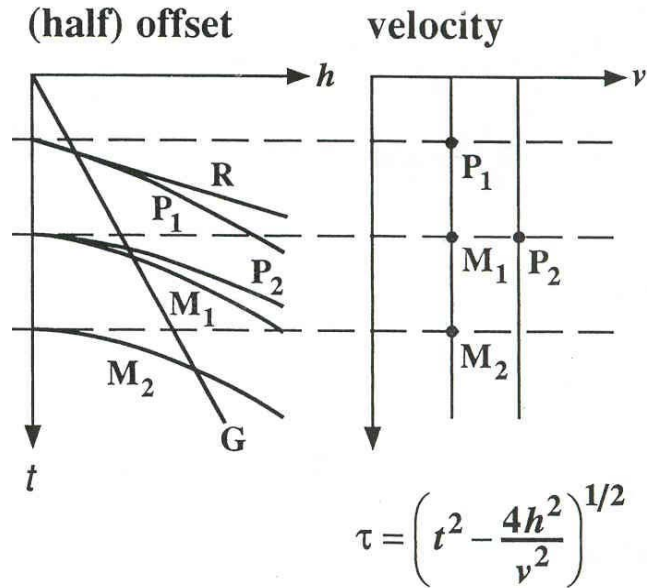


FIG. 4. Mapping from offset domain to velocity domain (Yilmaz, 1987)

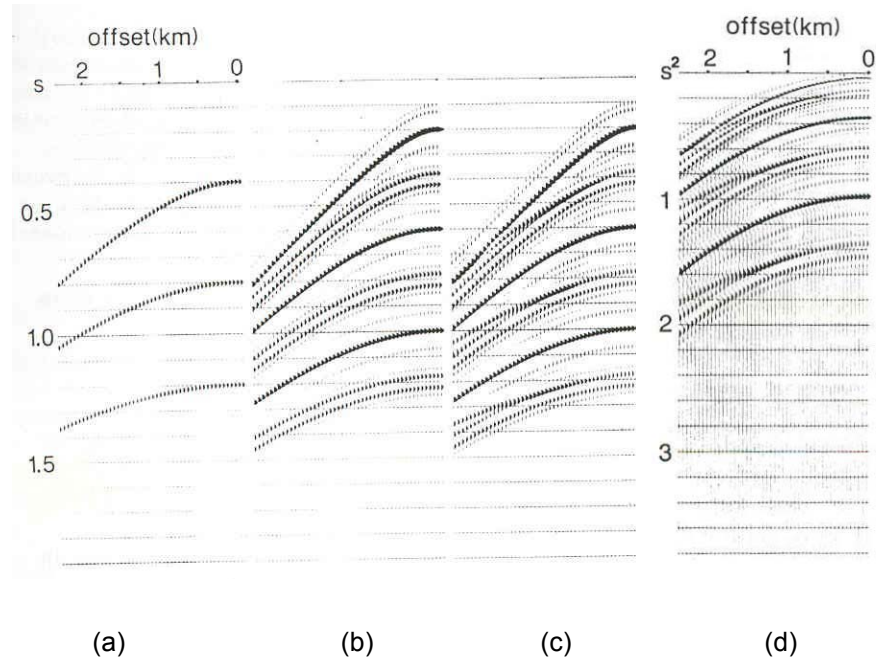


FIG. 5. (a) A synthetic CMP gather with three primary reflections; (b) A synthetic CMP gather with one primary reflection (arrival at 0.2 s at zero-offset) and its multiples; (c) Integration of (a) and (b); (d) t^2 -stretching section of (c) from Yilmaz (1987).

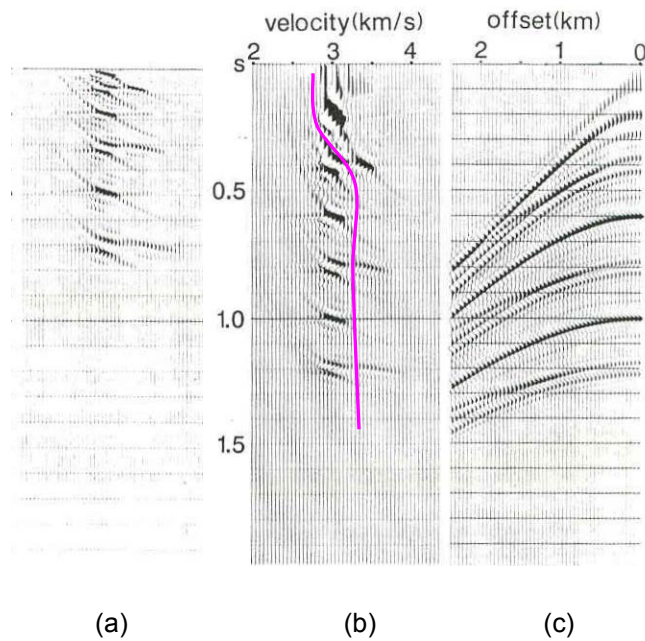


FIG. 6. (a) The velocity-stack of the CMP gather in Figure 5(d); (b) The velocity-stack after undo t^2 -stretching; (c) The CMP gather reconstructed from (b) given by Yilmaz (1989).

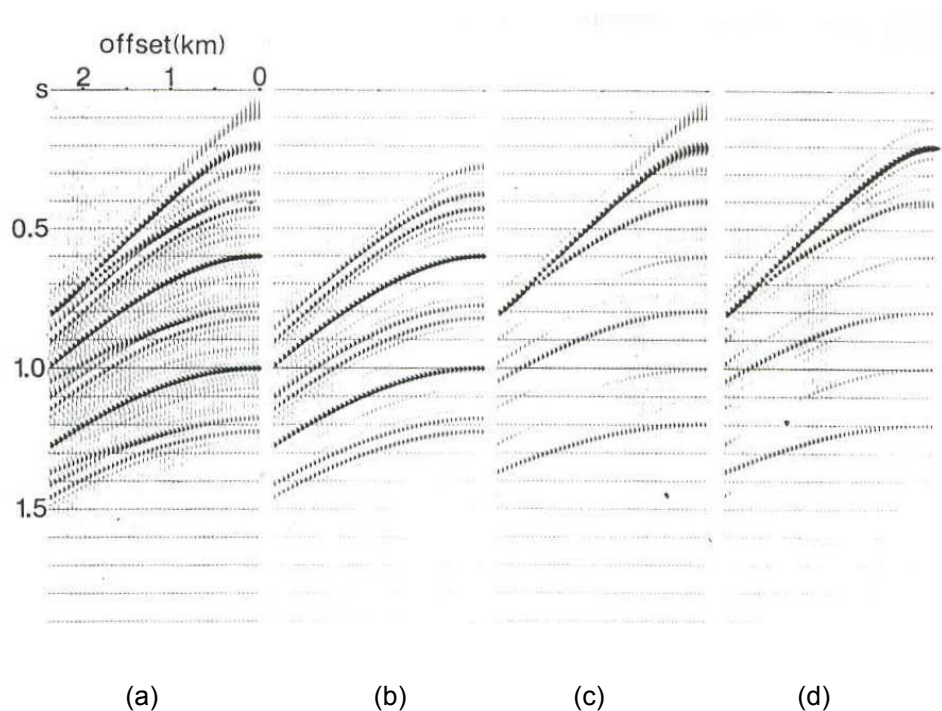


FIG. 7. (a) The reconstructed CMP gather from Figure 6b; (b) Only multiples constructed from Figure 6b; (c) Only primaries constructed from Figure 6b; (d) Subtraction of (b) from Figure 5c from Yilmaz (1989).

THE HYPERBOLIC RADON TRANSFORM

The Hyperbolic Radon Transform

A hyperbolic Radon transform performed on NMO-corrected gather, which is more correct than a parabola, was introduced by Foster and Mosher (1992). Foster and Mosher (1992) mentioned that there are two important conditions for keeping low cost of these computations. The first is that the stacking surface should be time-invariant so that computations may be performed in the frequency-space domain, and the second is that the matrix operators should have Toeplitz form so that fast solvers may be used.

Now we copy equation (1), the generalized Radon transform, as:

$$u(q, \tau) = \int_{-\infty}^{\infty} d(x, t = \tau + q\phi(x)) dx, \quad (69)$$

where d is the original seismic data, x is the offset, t is the two-way travelttime, u is the transform in model space, τ is the intercept time, and q is the curvature parameter.

Equation (69) is transformed to the frequency domain as:

$$U(q, \omega) = \int_{-\infty}^{\infty} D(x, \omega) e^{i\omega q \phi(x)} dx, \quad (70)$$

The summation along the curvature defined by parameter q , now becomes an integration of phase shifts in the frequency domain. The discrete form of equation (70) is:

$$U(q_j, \omega) = \sum_{k=1}^N D(x_k, \omega) e^{i\omega q_j \phi(x_k)} \Delta x_k, \quad (71)$$

Since multiples have hyperbolic moveout curves relative to traveltimes and offset distance, Foster and Mosher (1992) gave the factor of the time-delay function (phase shift) as follows:

$$\phi(x_k) = \sqrt{x_k^2 + z_{ref}^2} - z_{ref}, \quad (72)$$

where x_k is the offset receiver position and z_{ref} is a constant parameter defined as the reference depth. The choice of z_{ref} is not entirely arbitrary because the difference between these hyperbolae and those of reflected waves is controlled by this parameter. The smaller $\phi(x_k)$, the more compact the events will appear in the transform domain. With the value of z_{ref} , events reflected from this depth are optimally resolved.

The basic assumption of this method when applied to multiples suppression is that the moveout of multiples is different from that of the primaries.

The Shifted-Hyperbolic Radon Transform

Malovichko (1978) and Castle (1994) derived the shifted-hyperbolic NMO equation for a horizontally layered model as:

$$t = \tau_s + \sqrt{\tau_0^2 + \frac{h^2}{v^2}}, \quad (73)$$

where

$$\tau_s = \tau_0 + (S-1), \quad (74)$$

$$\tau_0 = \frac{t_0}{S}, \quad (75)$$

$$v^2 = SV_{rms}^2, \quad (76)$$

$$S = \frac{\mu_4}{\mu_2^2}, \quad (77)$$

$$\mu_n = \frac{\sum_{i=1}^N \Delta t_i V_i^n}{\sum_{i=1}^N \Delta t_i}, \quad (78)$$

The shifted-hyperbolic curve represents a Dix NMO equation shifted by the time τ_s and exact through fourth order in offset. Equation (73) can be written as:

$$t = t_0 + \sqrt{\frac{t_0^2 \mu_2^4}{\mu_4^2} + \frac{x^2 \mu_2^2}{\mu_4 V_{rms}^2}} - \frac{t_0 \mu_2^2}{\mu_4}, \quad (79)$$

or more simple:

$$t = t_0 - \frac{t_0}{S} + \sqrt{\left(\frac{t_0}{S}\right)^2 + \frac{x^2}{SV_{rms}^2}}, \quad (80)$$

With the summation curve of equation (80), the function $\phi(x)$ in equation (4) becomes (Oppert 2002):

$$\phi(x) = \sqrt{\frac{4z^2}{S^2} + \frac{x^2}{S} - \frac{2z}{S}}, \quad (81)$$

CONCLUSIONS

In the slant-stack domain, multiples are periodic for every p value. Predictive deconvolution can be applied in the slant-stack domain to suppress multiples. The parabolic Radon transform and the hyperbolic Radon transform can be performed to attenuating multiple based on the velocity discrimination. One of the problems associated with the Radon transform is that a CMP gather only includes a cable-length portion of a hyperbolic travelttime trajectory. The finite cable length will cause smearing of the

stacked amplitudes along the velocity axis. This can be overcome by a solution given by Thorson and Claerbout (1985).

COMMENTS

In Figure 6b, the CMP gather in the Radon domain doesn't have very good resolution. Another sample is shown in Figure 8, which is a common-scatter point (CSP) gather (real data from Alberta) and its velocity stack, which is a hyperbolic Radon transform that shows high resolution. The above principle of multiple attenuation will be applied to these types of CSP gathers formed by the equivalent offset method (EOM), Bancroft (1998). It is proposed that the improved focussing of CSP gathers, both spatially and temporally, will produce an improvement in the attenuation of multiples in prestack migrations.

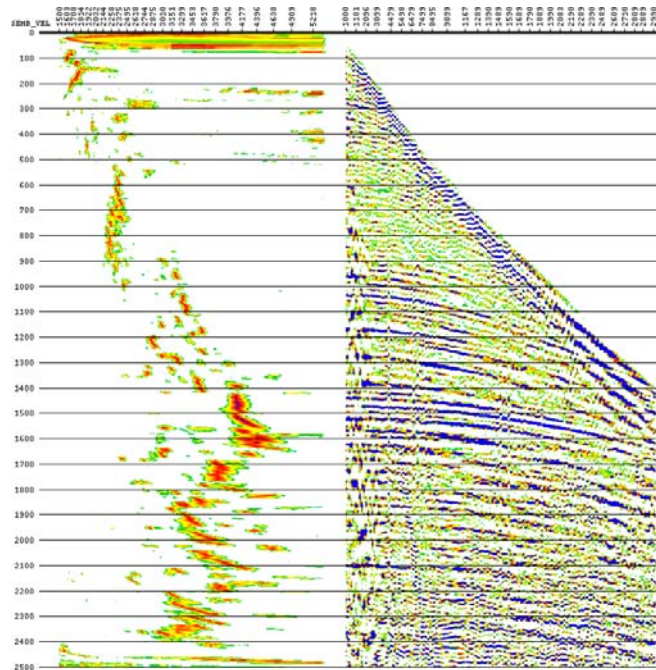


FIG. 8. Velocity stack or the hyperbolic Radon transform of a CSP gather (real data from Alberta) from Bancroft (2003).

ACKNOWLEDGEMENTS

Thanks to Dr. Bancroft and Dr. Brown for instruction, discussion, and suggestions. Thanks to the CREWES Project for funding this research.

REFERENCE

- Alam, A. and Austin, J., 1981, Suppression of multiples using slant stacks: 51st Ann. Internat. Mtg., Soc. Expl. Geophys., Expanded Abstracts, 3225-3257.
- Bancroft, J.C., Geiger, H.D., and Margrave, G.F., 1998, The equivalent offset method of prestack time migration: *Geophysics*, **63**, 2042-2053.
- Bancroft, J.C., 2003, A practical understanding of pre- and post-stack migration: SEG Course Notes.
- Beylkin, G., 1987, Discrete Radon transform: *IEEE Trans. Acoust., Speech, and Signal Proc.*, ASSP-35, No.2, 162-172.
- Castle, R. J., 1994, A theory of normal moveout: *Geophysics*, **20**, 68-86.
- Chapman, C.H., 1981, Generalized Radon transforms and slant stacks: *Geophys. J. R. Astr. Soc*, **66**, 445-453.
- Claerbout, J.F., 1985, *Imaging the Earth's Interior*: Blackwell Scientific Publications.
- Foster, D.J. and Mosher, C.C., 1992, Suppression of multiple reflections using the Radon transform: *Geophysics*, **57**, 386-395.
- Hampson, D., 1986, Inverse velocity stacking for multiple elimination: *J. Can. Soc. Expl. Geophys.*, **22**, 44-55.
- Malovichko, A.A., 1978, A new representation of the travelttime curve of reflected waves in horizontally layered media: *Applied Geophysics*, **91**, 47-53, (in Russian).
- Oppert, S.K., 2002, Radon methods for improved imaging of high-velocity layers using mode-converted energy: M.Sc. Thesis, Univ. of Calgary.
- Oppert, S.K. and Brown, R.J., 2002, Improved Radon transforms for filtering of coherent noise, CREWES Research Report, **14**.
- Taner, M.T., 1980, Long-period sea-floor multiples and their attenuation: *Geophys. Prosp.*, **28**, 30-48.
- Thorson, J.R. and Claerbout, J.F., 1985, Velocity-stack and slant-stack stochastic inversion: *Geophysics*, **50**, 2727-2741.
- Treitel, S., Gutowski, P.R., and Wagner, D.E., 1982, Plane-wave decomposition of seismograms: *Geophysics*, **47**, 1375-1401.
- Sacchi, M.D. and Tadeusz, J.U., 1995, High-resolution velocity gathers and offset space reconstruction: *Geophysics*, **60**, 1169-1177.
- Yilmaz, Ö., 1987, *Seismic Data Processing*: Soc. Expl. Geophys.
- Yilmaz, Ö., 1989, Velocity-stack processing: *Geophys. Prosp.*, **37**, 357-382.
- Yilmaz, Ö., 2001, *Seismic Data Processing*: Soc. Expl. Geophys.
- Zhou, B. and Greenhalgh, S.A., 1994, Linear and parabolic τ -p transforms revisited: *Geophysics*, **59**, 1133-1149.